

No Dynamic Changes in Inflammation-related Microcirculatory Parameters in Developing Rats During Local Cortex Exposure to Microwaves

HIROSHI MASUDA^{1,2}, SHOGO HIROTA², AKIRA USHIYAMA², AKIMASA HIRATA³,
TAKUJI ARIMA⁴, HIROKI KAWAI⁵, KANAKO WAKE⁵, SOICHI WATANABE⁵,
MASAO TAKI⁶, AKIKO NAGAI¹ and CHIYOJI OHKUBO⁷

¹*Institute of Biomaterials and Bioengineering, Tokyo Medical and Dental University, Tokyo, Japan;*

²*Department of Environmental Health, National Institute of Public Health, Saitama, Japan;*

³*Department of Computer Science and Engineering, Nagoya Institute of Technology, Aichi, Japan;*

⁴*Department of Electrical and Electronics Engineering,
Tokyo University of Agriculture and Technology, Tokyo, Japan;*

⁵*Electromagnetic Compatibility Laboratory, Applied Electromagnetic Research Institute,
National Institute of Information and Communications Technology, Tokyo, Japan;*

⁶*Department of Electrical and Electronic Engineering, Tokyo Metropolitan University, Tokyo, Japan;*

⁷*Japan EMF Information Center, Tokyo, Japan*

Abstract. *The biological effects of exposing the developing brain to radiofrequency electromagnetic fields (RF) are still unclear. Our experiments investigated whether three inflammation-related, microcirculatory parameters in juvenile and young adult rats were modified during local cortex exposure to RF under non-thermal conditions. The cortex tissue was locally exposed to 1457 MHz RF at an averaged specific absorption rate of 2.0 W/kg in the target area for 50 min and variations of pial venule parameter were measured directly in vivo. There was no significant difference in hemodynamics, plasma velocity or vessel diameter, between exposed and sham-exposed groups for either rat development stage. No increase related to RF exposure was found in leukocyte adhesion to endothelial cells in any microvessels observed. These findings suggest that RF is unlikely to initiate inflammatory responses, at least under these exposure conditions.*

In toxicological science, it is important to evaluate the adverse effects of physical and chemical factors on children's health

Correspondence to: H. Masuda, Ph.D., Institute of Biomaterials and Bioengineering, Tokyo Medical and Dental University, 2-3-10 Kanda-surugadai, Chiyoda-ku, Tokyo, ZIP 101-0062, Japan. Tel: +81 352808168, Fax: +81 352808015, e-mail: bdxmsd@yahoo.co.jp

Key Words: Radiofrequency electromagnetic field, local exposure, hemodynamics, plasma velocity, vessel diameter, leukocyte, adhesion, young adult rats, developing stage.

during their development. Sensitivity to certain factors is considered to be greater during the developmental stage than in adults. Many studies using experimental animals have suggested this tendency. For example, among physical factors, rat brains are known to exhibit age-dependent sensitivity to cellular injury caused by irradiation (1). Among chemical factors, ethanol has been reported to affect synaptic activity in the hippocampus, more severely, in developing rats than adults (2, 3). However, science and technology are constantly producing new physical and chemical factors with unknown toxicities. Therefore, toxicological evaluations during the developmental stage are recommended and several guidelines for developmental neurotoxicity testing are available (4, 5).

One physical factor recently considered likely to have an impact on health in the developmental stage is radiofrequency electromagnetic fields (RF). The intensity of RF is controlled under guidelines established by the International Commission on Non-Ionizing Radiation Protection to provide protection from known adverse health effects (6). The guidelines specify the basic restriction values in terms of specific absorption rates (SAR; W/kg). The restriction values for exposure of the general public to local and whole-body RF (100 kHz-10 GHz) are 2 and 0.08 W/kg, respectively. Nevertheless, recent use in various applications, such as magnetic resonance imaging and WiFi communications, has caused concern about possible adverse effects. In particular, widespread use of smartphones among the younger generation has accentuated this concern, leading to a requirement for early investigation into adverse effects at developmental stages (7).

Several research groups have evaluated the biological effects of RF exposure in rodents during the developmental stage (8-12), but the findings have not conclusively demonstrated adverse effects of RF under these conditions. In terms of the positive effects of RF, Paulraj and Behari found an increase in brain glial cell populations in rats at the developmental stage (35 to 70 days old) following chronic whole-body RF exposure at 0.11 W/kg (11). Kumlin *et al.* also reported that learning and memory in the water maze test were improved in developing rats after whole-body RF exposure for 5 weeks (9). In contrast, Klose *et al.* found that daily RF exposure of the rat head region had no harmful impact on learning skills or behavior, even in juveniles (8). Kuribayashi *et al.* also failed to find any adverse effects on the blood-brain barrier (BBB) of immature and young rats after local brain exposure to RF (10). Like these, the issue of the effects of RF during the developmental stage remains controversial.

If the brain were affected by RF exposure at the developmental stage, some possible effects might be observed as acute inflammatory responses. In pro-inflammatory and inflammatory situations in the brain, significant variations are known to occur in cerebral microcirculatory parameters, including vessel diameter, blood flow, leukocyte behavior, and permeability of the BBB (13-15). Previous experiments did not detect any acute effects of RF exposure on BBB permeability in developing rats (16), but no other parameters have been evaluated as far as we are aware of.

The aim of the present study was to investigate whether dynamic variations in hemodynamics and leukocyte behavior were observed in brains of juvenile and young adult rats during local cortex exposure to RF. Our group had already examined changes in these microcirculatory parameters in adult rats *in vivo* following RF exposure, but not in rats at developmental stages or during exposure.

Materials and Methods

Animals. Male Sprague-Dawley rats of two different ages, 4-week-old juvenile rats ($n=31$, 128 ± 4 g) and 8-week-old young adult rats ($n=36$, 327 ± 5 g), (Japan SLC, Inc., Shizuoka, Japan) were used for this experiment. They were fed a standard pellet diet and given water *ad libitum* in an animal room with a 12-h light/dark cycle at a temperature of $23.0\pm1^\circ\text{C}$ and a relative humidity of $50\pm10\%$. All experimental procedures were conducted in accordance with the ethical guidelines for animal experiments at the National Institute of Public Health, Japan.

Preparation of closed cranial window. The closed cranial window setup (CCW) was implanted into the parietal region of each rat at least one week before the observation. The CCW was previously developed to observe dynamic changes in pial microcirculatory parameters, such as BBB function and plasma velocity under RF exposure conditions (17-19). In brief, the rats were anesthetized with an intramuscular injection of ketamine (100 mg/kg) and xylazine (10 mg/kg). After removal of skin, connective tissues and a 7.5-mm

circular patch of skull from the parietal region, the CCW (circular cover-glass 7.0 mm in diameter) was inserted into the hole in the skull and fixed with acrylic glue.

Definition of target area and local RF exposure. The target cortex tissue was locally exposed to a 1457 MHz RF (signal type; Personal Digital Cellular signal) at several averaged SAR for the target cortex, using a figure-8 loop antenna positioned 5 mm above the CCW (20, 21) (Figure 1A).

The target area was defined as a diskoid area of rat parietal cortex tissue, located just under the CCW, centered 1.5 mm posterior of the bregma and 1.5 mm lateral (left) of the midline. The area included the *pia mater* (7.5 mm diameter, 0.5 mm depth), in which physiological responses were evaluated during local RF exposure (Figure 1B).

RF exposure intensities were estimated and set at 2.0 W/kg SAR in the target area (TASAR) for rats of both age groups. For juvenile rats, the relative values of brain- and whole body-averaged SARs for the TASAR of 2.0 W/kg were 0.59 and 0.057 W/kg, respectively. For young adult rats, these averaged SARs were 0.54 and 0.03 W/kg, respectively. Exposure at 2.0 W/kg continued for 50 min in order to record changes in microcirculatory parameters. The sham-exposed rats were also prepared using the same system, but without RF exposure (0 W/kg).

Real-time measurement of microcirculatory parameters. Three microcirculatory parameters were measured before, during, and immediately after RF exposure (Figure 1C), using an intravital fluorescence microscopy system built for previous experiments (21). In brief, rats were anesthetized with an intramuscular injection of ketamine (100 mg/kg) and xylazine (10 mg/kg) and a subcutaneous injection of pentobarbital (12.5 mg/kg). Each rat was placed on a heating pad circulating warmed water (42°C) during exposure.

Monitoring was carried-out through the CCW using intravital fluorescence microscopy. The system used for observing the two hemodynamic parameters consisted of a binocular fluorescence microscope (SZX12; Olympus Optical Co. Ltd., Tokyo, Japan), an EB-CCD camera (C7190-23; Hamamatsu Photonics K.K., Hamamatsu, Japan), and high-speed camera (FASTCAM-NET; Photron Ltd., Tokyo, Japan), combined with an image-intensifier (VS4-1845; International Ltd., Dulles, VA, USA). The other parameter, leukocyte behavior, was monitored using a binocular fluorescence microscope (MVX10; Olympus Optical Co. Ltd.) and the EB-CCD camera. Two fluorescence dyes, fluorescein isothiocyanate (FITC)-dextran for hemodynamics (70 kDa, 25 mg/kg; Sigma-Aldrich Co., St. Louis, MO, USA) and Rhodamine 6G (100 $\mu\text{g/kg}$; Sigma-Aldrich Co.) were intravenously injected to visualize the plasma and leukocytes, respectively, in pial venules. The fluorescence images of the pial microvascular bed were captured on a video recorder (WV-DR7; Sony, Tokyo, Japan) equipped with a timer (VTG-33; FOR.A Co. Ltd., Tokyo, Japan). All images were later analyzed off-line.

Observation of hemodynamics. To evaluate the hemodynamics in the pial venule, its diameter and blood flow velocity were measured using the method reported previously (17, 21). In brief, venule diameter was measured on the fluorescence images every 10 min after the FITC-dextran injection. In each animal, 7-12 pial venules ($8 \leq d \leq 50 \mu\text{m}$) were selected and the ratio of the venule diameter to the initial diameter at 10 min before exposure was recorded. Blood flow velocity was measured using the dual-slit method developed by our

team (22). The fluorescence motion images of blood flow in the pial venule were recorded using a high-speed camera (500 frames/s) every 10 min after the intravenous FITC-dextran injection. Blood flow velocity was calculated using the time interval obtained from dual-slit intensity and the distance between the two slits. We selected 4–12 pial venules ($8 \leq d \leq 50 \mu\text{m}$) in each animal and recorded the ratio of the velocity to the initial velocity at 10 min before exposure. Variations in diameter and velocity were averaged for each animal to obtain the average change within the target area for the animal and then compared between sham- and RF-exposed groups ($n=6$ –14 animals per each group).

Observation of leukocyte behavior. Changes in leukocyte behavior were evaluated using the number of leukocytes that interacted with the endothelium of the pial venules (18). In brief, the interactions were classified into one of two states as 'rolling' or 'sticking'. Rolling leukocytes were defined as cells that interacted weakly with the endothelium and exhibited a rolling behavior along its surface. Sticking leukocytes were defined as cells that attached to the endothelium for at least 30 s with strong interactions. Leukocytes were visualized with Rhodamine 6G and measured on the fluorescence images for 30 s per venule. The number of leukocytes in each state was counted on a 100- μm length of the pial venules.

Positive control. To confirm that the observation methods were valid, a phototoxic injury model (23) of rat cerebral microcirculation was prepared as a positive control. A juvenile rat, which had been observed for evaluating leukocyte behavior under sham exposure conditions, was reused for this purpose. The pial microvascular bed was exposed to a maximum intensity light source (488 nm) through the CCW for 90 s after intravenous injection of FITC-dextran. Venular diameter and leukocyte behavior were observed using fluorescence microscopy, as described above.

Data analysis. Two-way repeated ANOVA and the Mann–Whitney *U*-test were used for statistical analysis to evaluate the differences between the sham- and RF-exposed groups. A value of $p < 0.05$ was considered statistically significant.

Results

Temperature conditions. Details of temperature conditions for this experiment were described in our companion article (16). The temperature information is, therefore, repeated briefly here for reference: Basal temperatures in the target area and rectum at the beginning of exposure were stabilized, without any significant difference between sham- and RF-treated groups ($n=3$ animals per group). In juvenile rats, the average temperatures in the target area in sham- and RF-treated groups were $34.6 \pm 1.1^\circ\text{C}$ and $35.1 \pm 0.8^\circ\text{C}$, respectively. The average rectal temperatures were $35.4 \pm 0.3^\circ\text{C}$ and $36.1 \pm 0.7^\circ\text{C}$, respectively. Similar results were obtained in young adult rats, with average target area temperatures of $34.7 \pm 0.3^\circ\text{C}$ and $35.0 \pm 0.1^\circ\text{C}$, and rectal temperatures of $36.2 \pm 0.3^\circ\text{C}$ and $36.2 \pm 0.1^\circ\text{C}$, respectively. There were no significant differences in either basal temperature between the two exposed groups. In addition, these data confirmed that local 50-min RF exposure at 2.0 W/kg did not cause any increase in temperature.

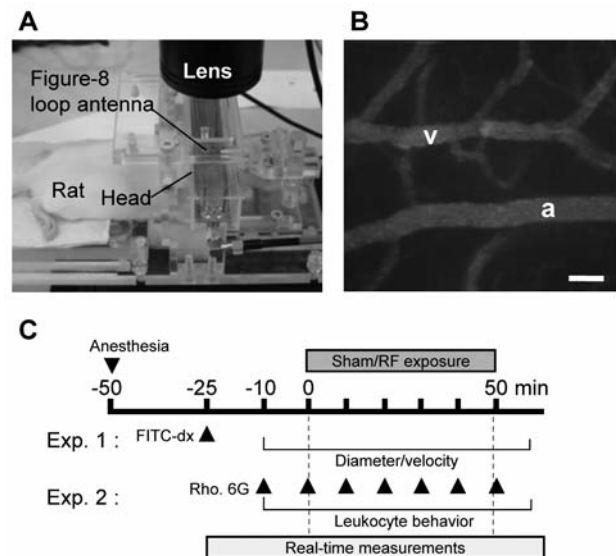


Figure 1. Experimental design. A: Set up for radiofrequency electromagnetic field (RF) exposure and observation. A closed cranial window was implanted over the target area through the open skull. The antenna was placed over the parietal region using a manipulator. Rat pial microcirculation was observed in real-time through holes in the antenna, using intravital microscopy. B: Overview of the pial microvessels under a fluorescence microscope. The vessels were visualized using fluorescein isothiocyanate-dextran (FITC-dextran). a: Arteriole, v: venule. Bar: 100 μm . C: Experimental procedure. Two fluorescence dyes, FITC-dextran and Rhodamine 6G (Rho. 6G), were used to observe hemodynamics and leukocyte behavior, respectively. Each dye was injected via the rat tail vein before the real-time measurements.

Hemodynamic variations. To determine whether cerebral hemodynamics were modified under local RF exposure, vessel diameter and blood flow velocity in the pial venules were measured as hemodynamic parameters during local RF exposure at 2.0 W/kg TASAR.

In juvenile rats, a slight dilation of the pial venules was observed during exposure (Figure 2A). However, there was no significant difference in this parameter between sham- (124 venules in 11 animals) and RF- (113 venules in 10 animals) treated groups throughout the experiment. Similar results were obtained in young adult rats (Figure 2B). No significant difference in venule diameter was found between sham- (129 venules in 11 animals) and RF- (166 venules in 14 animals) treated groups. These results revealed that no change in venule diameter was caused by local RF exposure at 2.0 W/kg TASAR, even in animals in the developmental stage.

Blood flow velocity in the pial venules of juvenile rats increased during exposure (Figure 3A). However, there was no significant difference in this parameter between sham- (86 venules in eight animals) and RF- (55 venules in six animals)

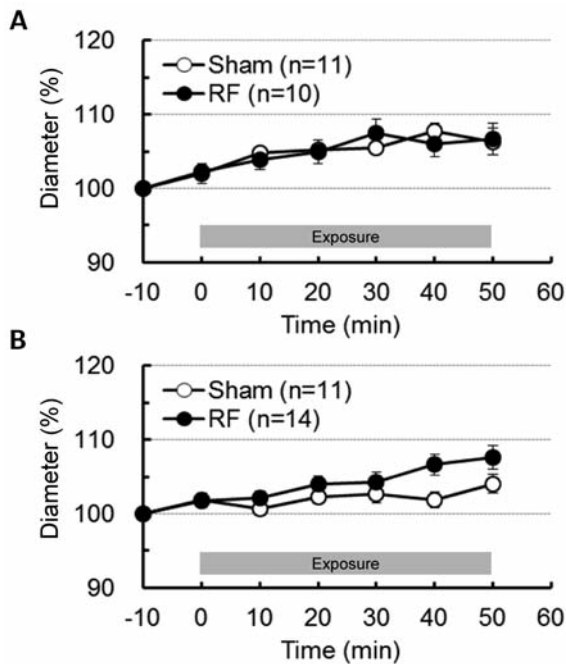


Figure 2. Effects of radiofrequency electromagnetic field (RF) exposure on pial venular diameter. The diameter of the pial venules ($8 \leq d < 50 \mu\text{m}$) within the target area was measured before, during, and just after RF exposure. There were no significant differences between the sham- and RF-exposed groups of juvenile rats (A) or young adult rats (B). Values are the mean \pm SEM.

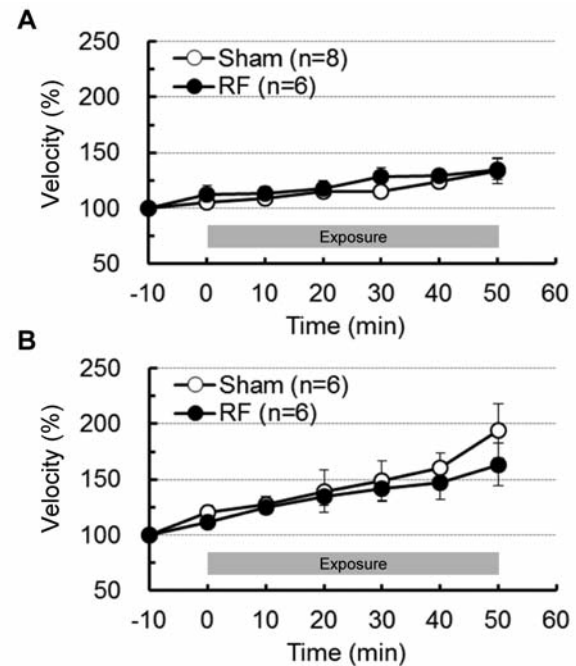


Figure 3. Effects of radiofrequency electromagnetic field (RF) exposure on plasma velocity in pial venules. Plasma velocity was measured in the pial venules ($8 \leq d < 50 \mu\text{m}$) in the target area before, during, and just after RF exposure. There were no significant differences between the sham- and RF-exposed groups of juvenile rats (A) or young adult rats (B). Values are the mean \pm SEM.

treated groups throughout the experiment. An increase in blood flow velocity was also observed in young adult rats (Figure 3B), during exposure. However, there was no significant difference in the velocity change between sham- (65 venules in six animals) and RF-treated (68 venules in six animals) groups throughout the experiment. Results revealed that local RF exposure at 2.0 W/kg did not cause any change in blood flow velocity in the pial venules, even in animals in the developmental stage.

Leukocyte behavior. To evaluate leukocyte behavior in the cerebral target area during local RF exposure at 2.0 W/kg TASAR, we measured the number of leukocytes interacting with the endothelium in pial venules (Figure 4). In juvenile rats, no significant adhesion of leukocytes was observed in pial venules during RF exposure. Both rolling and sticking leukocytes were counted in 30 venules in five animals of each group. However, there was no significant difference in adhesive behavior between sham- and RF-treated groups throughout the experiment. Similar results were obtained in young adult rats. These results revealed that local RF exposure at 2.0 W/kg TASAR caused no change in adhesive behavior of leukocytes even at developmental stages.

Discussion

This *in vivo* study using real-time observation in juvenile and young adult rats produced two main findings under non-thermal exposure conditions. Firstly, the local RF exposure used for a target cortex area at 2.0 W/kg TASAR did not affect hemodynamics of pial venules in the target area throughout the experiment in rats of either age. Secondly, no increase in leukocyte adhesiveness to venular endothelial cells occurred during the exposure in any targets we observed.

We firstly focused on hemodynamics as an inflammation-related microcirculatory parameter. Under pro-inflammatory or inflammatory conditions in the brain, microvascular blood flow and diameter, which are key elements of hemodynamics, are known to change. Using the rat stroke model, for example, Ritter *et al.* found that the mean velocity of leukocytes flowing in cerebral venules was reduced through the reperfusion period (15). For microvascular diameter, several inflammatory mediators such as lipopolysaccharide (13, 24), vascular endothelial growth factor (25) and histamine (26), were found to modify microvascular tone after their administration. Our observation method using intravital microscopy confirmed pial venular dilation in the cerebral microvascular bed under

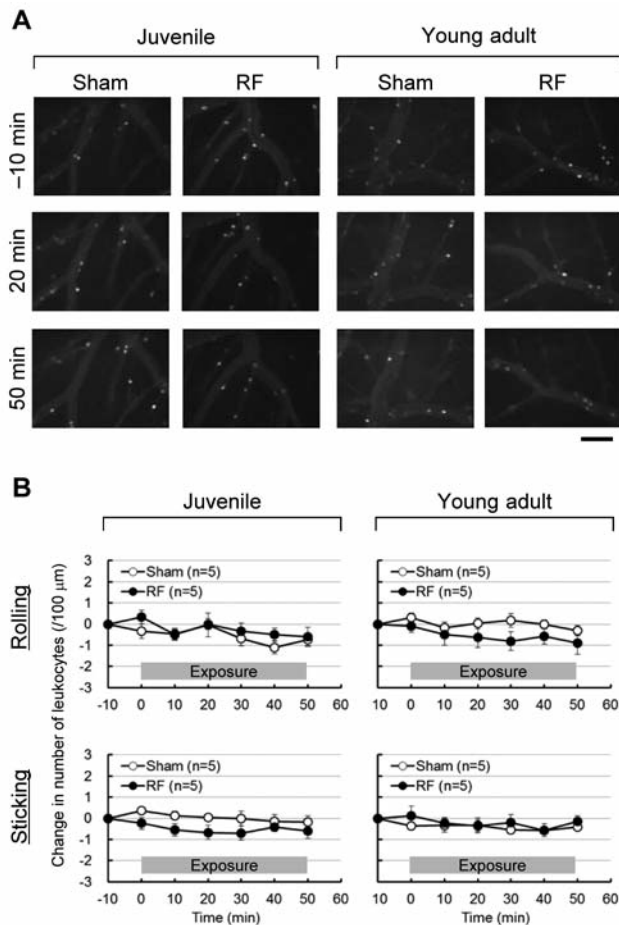


Figure 4. Effects of radiofrequency electromagnetic field (RF) exposure on leukocyte behaviors in pial venules. A: Representative fluorescence images of the pial microvascular bed in the target area during each time period. Rhodamine 6G was intravenously injected into the rats before each observation to visualize leukocytes (white cells). Bar: 100 μ m. B: The number of rolling and sticking leukocytes (per 100 μ m in length) in the pial venules ($8 \leq d < 50 \mu$ m) within the target area was counted before, during, and just after RF exposure. There were no significant differences in either type of leukocyte behavior between the sham- and RF-exposed groups of juvenile or young adult rats. Values are the mean \pm SEM.

inflammatory conditions induced by phototoxic injury (Figure 5A and B). Therefore, if inflammatory responses were caused by RF exposure, these hemodynamic changes would be detected in the brain during RF exposure. However, dynamic changes related to RF occurred, neither in blood flow velocity nor in diameter in pial venules throughout our experiments, including the exposure period of 50 min. In addition, no dynamic changes in these parameters were found in target areas of rats of either age group. Our previous study confirmed similar results in 14-week-old adult rats under the same exposure conditions (21). Therefore, these findings suggest that there was no difference between juvenile and adult rats in

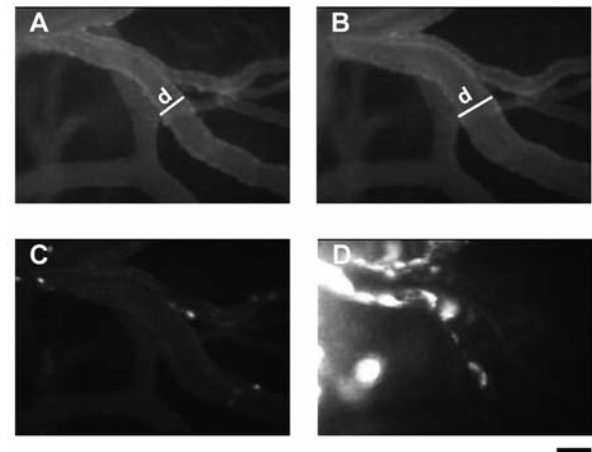


Figure 5. Positive control for intravital microscopic evaluation. A positive control for venular diameter (A, B) and leukocyte adhesiveness (C, D) was obtained using a juvenile rat phototoxic injury model with a high intensity light source. Pial venules, visualized with fluorescein isothiocyanate-dextran, had dilated after 90 s light exposure (B, $d=68 \mu$ m), compared to the same venules before exposure (A, $d=49 \mu$ m). Adhesiveness of leukocytes, visualized with Rhodamine 6G, increased in the venular lumens 100 s after light exposure (D), compared with the venular lumens just after exposure (C). Bar: 50 μ m.

terms of the effects of RF exposure on microvascular hemodynamics in the brain.

The second inflammation-related parameter we focused was leukocyte behavior. Leukocyte behavior is a good indicator for evaluating the phase of pro-inflammatory or inflammatory responses in cerebral tissues (15, 27). Inflammation is known to increase adhesiveness between leukocytes and cerebrovascular endothelial cells, resulting in leukocytes rolling and sticking behavior (28, 29). An increase in rolling behavior is initiated by pro-inflammatory conditions. Exacerbation of inflammatory conditions increases the number of rolling leukocytes, as well as initiating sticking behavior, which affects endothelial and other cells, such as neuronal/glial cells, located around microvessels (28). Indeed, an increase in the number of rolling and sticking leukocytes was observed in brain treated with several inflammatory mediators (30-32). Our observations confirmed an increase in leukocyte adhesiveness in the phototoxic brain model (Figure 5C, D). Previous experiments using adult rats already found that no modification in leukocyte adhesiveness was observed after either a 10-min exposure at 4.8 W/kg of brain averaged SAR (BASAR) (18) or a 4-week exposure at 2.4 W/kg of BASAR (19). However, it was still unclear whether dynamic variations in leukocyte behavior occurred during RF exposure, which was likely to appear only as a transient phenomenon. This experiment was designed to reveal dynamic changes in leukocyte adhesiveness to venular endothelial cells in real-time during RF exposure, localized in target cortex tissue. However, leukocyte

behavior did not indicate any inflammatory reactions during or after 50-min RF exposure in either juvenile or young adult rats. These findings suggested that RF exposure below the local limit (2 W/kg) was unlikely to cause pro-inflammatory/inflammatory responses in rat brain of either age.

One of the most cited effects of brain exposure to RF is BBB disruption. While a few research groups found albumin leakage sites in rodent brains following RF exposure (33, 34), many other groups have failed to confirm this phenomenon under controlled experimental conditions (35-40). Furthermore, recent histological studies also revealed that no BBB disruption occurred following RF exposure, even in animals in the developmental stage (10, 41). The findings reported here strongly support the results showing no effect on the BBB, as permeability changes in the BBB are considered to be closely related to microvascular hemodynamics and leukocyte adhesiveness to venular endothelial cells under inflammatory conditions. For example, under inflammatory conditions induced by administering lipopolysaccharide, rat brain pial venules were observed to dilate prior to an increase in BBB permeability (13). In addition, many studies have reported that BBB disruption frequently occurs simultaneously with or after an increase in leukocyte adhesiveness (27, 42). Indeed, in the positive control brain subjected to phototoxic inflammation, extravasation of FITC-dextran was finally observed after both venular dilation and an increase in leukocyte adhesiveness (data not shown). Therefore, if BBB permeability increases due to RF exposure, changes in hemodynamics or leukocyte behaviors should be observed prior to the BBB disruption. However, no modification of these microcirculatory parameters was detected in this study. In fact, under the same experimental conditions described herein, no change in BBB permeability was confirmed in our companion study (16). All findings considered, these results may provide evidence to support the absence of any effect of RF exposure on BBB permeability.

Conflicts of Interest

The Authors have declared that they have no competing interests in regard to this study.

Acknowledgements

This study was financially supported by the Ministry of Internal Affairs and Communications, Japan. The Authors would like to thank Mrs. Miyuki Takahashi, Kasumi Yamanaka, and Minako Segawa for their helpful assistance.

References

- Fukuda A, Fukuda H, Swanpalmer J, Hertzman S, Lannering B, Marky I, Björk-Eriksson T and Blomgren K: Age-dependent sensitivity of the developing brain to irradiation is correlated with the number and vulnerability of progenitor cells. *J Neurochem* 92: 569-584, 2005.
- Pyapali GK, Turner DA, Wilson WA and Swartzwelder HS: Age and dose-dependent effects of ethanol on the induction of hippocampal long-term potentiation. *Alcohol* 19: 107-111, 1999.
- Swartzwelder HS, Wilson WA and Tayyeb MI: Differential sensitivity of NMDA receptor-mediated synaptic potentials to ethanol in immature versus mature hippocampus. *Alcohol Clin Exp Res* 19: 320-323, 1995.
- Hass U: Current status of developmental neurotoxicity: regulatory view. *Toxicology Letters* 140-141: 155-159, 2003.
- Hass U: The need for developmental neurotoxicity studies in risk assessment for developmental toxicity. *Reprod Toxicol* 22: 148-156, 2006.
- International Commission on Non-Ionizing Radiation Protection: Guidelines for limiting exposure to time-varying electric, magnetic, and electromagnetic fields (up to 300 GHz). *Health Phys* 74: 494-522, 1998.
- World Health Organization 2010: WHO research agenda for radiofrequency fields. http://whqlibdoc.who.int/publications/2010/9789241599948_eng.pdf, 2010
- Klose M, Grote K, Spathmann O, Streckert J, Clemens M, Hansen VW and Lerchl A: Effects of early-onset radiofrequency electromagnetic field exposure (GSM 900 MHz) on behavior and memory in rats. *Radiat Res* 182: 435-447, 2014.
- Kumlin T, Iivonen H, Miettinen P, Juvonen A, van Groen T, Puranen L, Pitkäaho R, Juutilainen J and Tanila H: Mobile phone radiation and the developing brain: behavioral and morphological effects in juvenile rats. *Radiat Res* 168: 471-479, 2007.
- Kuribayashi M, Wang J, Fujiwara O, Doi Y, Nabae K, Tamano S, Ogiso T, Asamoto M and Shirai T: Lack of effects of 1439 MHz electromagnetic near field exposure on the blood-brain barrier in immature and young rats. *Bioelectromagnetics* 26: 578-588, 2005.
- Paulraj R and Behari J: Protein kinase C activity in developing rat brain cells exposed to 2.45 GHz radiation. *Electromagn Biol Med* 25: 61-70, 2006.
- Watilliaux A, Edeline J-M, Lévêque P, Jay TM and Mallat M: Effect of exposure to 1,800 MHz electromagnetic fields on heat-shock proteins and glial cells in the brain of developing rats. *Neurotox Res* 20: 109-119, 2011.
- Ruiz-Valdepeñas L, Martínez-Orgado JA, Benito C, Millán Á, Tolón RM and Romero J: Cannabidiol reduces lipopolysaccharide-induced vascular changes and inflammation in the mouse brain: an intravital microscopy study. *J Neuroinflammation* 8: 5, 2011.
- Altura BM, Gebrewold A, Zhang A and Altura BT: Role of leukocytes in ethanol-induced microvascular injury in the rat brain *in situ*: potential role in alcohol brain pathology and stroke. *Eur J Pharmacol* 448: 89-94, 2002.
- Ritter LS, Orozco JA, Coull BM, McDonagh PF and Rosenblum WI: Leukocyte accumulation and hemodynamic changes in the cerebral microcirculation during early reperfusion after stroke. *Stroke* 31: 1153-1161, 2000.
- Masuda H, Hirota S, Ushiyama A, Hirata A, Arima T, Kawai H, Wake K, Watanabe S, Taki M, Nagai A and Ohkubo C: No dynamic changes in blood-brain barrier permeability occur in developing rats during local cortex exposure to microwaves. *In Vivo* 29: 351-357, 2015.
- Masuda H, Ushiyama A, Hirota S, Lawlor GF and Ohkubo C: Long-term observation of pial microcirculatory parameters using an implanted cranial window method in the rat. *In Vivo* 21: 471-479, 2007.

- 18 Masuda H, Ushiyama A, Hirota S, Wake K, Watanabe S, Yamanaka Y, Taki M and Ohkubo C: Effects of acute exposure to a 1439 MHz electromagnetic field on the microcirculatory parameters in rat brain. *In Vivo* 21: 555-562, 2007.
- 19 Masuda H, Ushiyama A, Hirota S, Wake K, Watanabe S, Yamanaka Y, Taki M and Ohkubo C: Effects of subchronic exposure to a 1439 MHz electromagnetic field on the microcirculatory parameters in rat brain. *In Vivo* 21: 563-570, 2007.
- 20 Arima T, Watanabe H, Wake K, Masuda H, Watanabe S, Taki M and Uno T: Local exposure system for rats head using a figure-8 loop antenna in 1500-MHz band. *IEEE Trans Biomed Eng* 58: 2740-2747, 2011.
- 21 Masuda H, Hirota S, Ushiyama A, Hirata A, Arima T, Watanabe H, Wake K, Watanabe S, Taki M, Nagai A and Ohkubo C: No changes in cerebral microcirculatory parameters in rat during local cortex exposure to microwaves. *In Vivo* 29: 207-215, 2015.
- 22 Hirota S, Masuda H, Ushiyama A, Asano M and Ohkubo C: Dual-slit photometric measurement of blood flow velocity by direct plasma fluorescence in rat pial microvessels. *Microcirculation Annual*. M. Asano and T. Tamamoto (eds.). Nihon-Igakukan, Tokyo, Japan pp. 95-96, 2004.
- 23 Rumbaut RE and Sial AJ: Differential phototoxicity of fluorescent dye-labeled albumin conjugates. *Microcirculation* 6: 205-213, 1999.
- 24 Mayhan WG: Effect of lipopolysaccharide on the permeability and reactivity of the cerebral microcirculation: role of inducible nitric oxide synthase. *Brain Res* 792: 353-357, 1998.
- 25 Mayhan WG: VEGF increases permeability of the blood-brain barrier via a nitric oxide synthase/cGMP-dependent pathway. *Am J Physiol* 276: C1148-53, 1999.
- 26 Mayhan WG: Role of nitric oxide in histamine-induced increases in permeability of the blood-brain barrier. *Brain Res* 743: 70-76, 1996.
- 27 Ishikawa M, Vowinkel T, Stokes KY, Arumugam TV, Yilmaz G, Nanda A and Granger DN: CD40/CD40 ligand signaling in mouse cerebral microvasculature after focal ischemia/reperfusion. *Circulation* 111: 1690-1696, 2005.
- 28 Gavins FNE, Hughes EL, Buss NAPS, Holloway PM, Getting SJ and Buckingham JC: Leukocyte recruitment in the brain in sepsis: involvement of the annexin 1-FPR2/ALX anti-inflammatory system. *FASEB J* 26: 4977-4989, 2012.
- 29 Kubes P and Kerfoot SM: Leukocyte recruitment in the microcirculation: the rolling paradigm revisited. *News Physiol Sci* 16: 76-80, 2001.
- 30 Waldner MJ, Baethmann A, Uhl E and Lehmberg J: Bradykinin-induced leukocyte- and platelet-endothelium interactions in the cerebral microcirculation. *Brain Res* 1448: 163-169, 2012.
- 31 Altura BM and Gebrewold A: Inhibitor of nuclear factor-kappa B activation attenuates venular constriction, leukocyte rolling-adhesion and microvessel rupture induced by ethanol in intact rat brain microcirculation: relation to ethanol-induced brain injury. *Neurosci Lett* 334: 21-24, 2002.
- 32 Vergnolle N, Derian CK, D'Andrea MR, Steinhoff M and Andrade-Gordon P: Characterization of thrombin-induced leukocyte rolling and adherence: a potential proinflammatory role for proteinase-activated receptor-4. *J Immunol* 169: 1467-1473, 2002.
- 33 Salford LG, Brun A, Stureson K, Eberhardt JL and Persson BR: Permeability of the blood-brain barrier induced by 915 MHz electromagnetic radiation, continuous wave and modulated at 8, 16, 50, and 200 Hz. *Microsc Res Tech* 27: 535-542, 1994.
- 34 Sirav B and Seyhan N: Blood-brain barrier disruption by continuous-wave radio frequency radiation. *Electromagn Biol Med* 28: 215-222, 2009.
- 35 De Gannes FP, Billaudel B, Taxile M, Haro E, Ruffie G, Leveque P, Veyret B and Lagroye I: Effects of head-only exposure of rats to GSM-900 on blood-brain barrier permeability and neuronal degeneration. *Radiat Res* 172: 359-367, 2009.
- 36 McQuade JM, Merritt JH, Miller SA, Scholin T, Cook MC, Salazar A, Rahimi OB, Murphy MR and Mason PA: Radiofrequency-radiation exposure does not induce detectable leakage of albumin across the blood-brain barrier. *Radiat Res* 171: 615-621, 2009.
- 37 Masuda H, Ushiyama A, Takahashi M, Wang J, Fujiwara O, Hikage T, Nojima T, Fujita K, Kudo M and Ohkubo C: Effects of 915 MHz electromagnetic-field radiation in TEM cell on the blood-brain barrier and neurons in the rat brain. *Radiat Res* 172: 66-73, 2009.
- 38 Tsurita G, Nagawa H, Ueno S, Watanabe S and Taki M: Biological and morphological effects on the brain after exposure of rats to a 1439 MHz TDMA field. *Bioelectromagnetics* 21: 364-371, 2000.
- 39 Finnie JW, Blumbergs, P. C., Manavis J, Utteridge TD, Gebiski V, Swift JG, Vernon Roberts B and Kuchel TR: Effect of global system for mobile communication (GSM)-like radiofrequency fields on vascular permeability in mouse brain. *Pathology* 33: 338-340, 2001.
- 40 Finnie JW, Blumbergs, P. C., Manavis J, Utteridge TD, Gebiski V, Davies RA, Vernon Roberts B and Kuchel TR: Effect of long-term mobile communication microwave exposure on vascular permeability in mouse brain. *Pathology* 34: 344-347, 2002.
- 41 Finnie JW, Blumbergs PC, Cai Z, Manavis J and Kuchel TR: Neonatal mouse brain exposure to mobile telephony and effect on blood-brain barrier permeability. *Pathology* 38: 262-263, 2006.
- 42 Yuan H, Gaber MW, McColgan T, Naimark MD, Kiani MF and Merchant TE: Radiation-induced permeability and leukocyte adhesion in the rat blood-brain barrier: modulation with anti-ICAM-1 antibodies. *Brain Res* 969: 59-69, 2003.

Received June 1, 2015

Revised July 13, 2015

Accepted July 15, 2015